

NUMERICAL COMPARISON OF SECOND-MOMENT CLOSURE MODELLING WITH DNS FOR NEAR-WALL SUB-LAYER OF TURBULENCE

L. Yu

*University of São Paulo, EESC
Department of Hydraulics and Sanitary Engineering
13570-970, São Carlos, Brazil*

A.M. Righetto

*University of São Paulo, EESC
Department of Hydraulics and Sanitary Engineering
13570-970, São Carlos, Brazil*

ABSTRACT. The second-moment closure model (Reynolds Stress Model – RSM) are high-class and refined multi-equation closure models of turbulence with higher precision, more complexity and stronger ability in simulation and prediction than the conventional two-equations closure models of turbulence. Theoretically, the RSM, which directly close the Reynolds-Stress Tensor (RST), have great potential and encouraging prospects to be adopted for modelling industrial and engineering problems. However, the development and application of second-moment closure models now are still in the primary stage, because of their great complexity and also of the difficulty to model the near-wall sub-layer of turbulence. The simplified wall treatment, such as the commonly used wall-function approximation, can not efficiently simulate the complex effects of wall. Further investigations of the high-class stress/flux-equation models are in urgent need, especially to extend the second-moment closure to the near-wall sub-layer of turbulence. Due to the recent progress of Direct Numerical Simulation (DNS), it has become possible to test turbulence models at the level of Reynolds stress budgets in simple shear flows. This paper presents the numerical comparison between the computational results of modelling near-wall sub-layer of turbulence by using the Launder and Shima's (L&S-Model, 1989) second-moment closure model and those resulted from DNS for the classical flat-plate boundary layer flow.

Key words: *Reynolds stress model, second-moment closure, boundary layer flow, near-wall sub-layer, Direct Numerical Simulation.*

1. INTRODUCTION

Based on the widely adopted Reynolds decomposition, the non-linear convection processes lead to the appearance of time-averaged products of fluctuating velocities, *i.e.* the turbulent stresses (Reynolds stresses) $-\rho \overline{u_i v_j}$, that are unknown in the Reynolds equation. The approximate representation of these terms in terms of known or calculable quantities is known as turbulence closure or turbulence modelling.

Most of the practically used turbulence models at present are based on the well-known, frequently used Boussinesq's eddy viscosity/diffusivity concept. The eddy viscosity concept, relating the Reynolds stresses to the mean velocity gradients, assumes on analogy between the momentum transport by the turbulent motion and the transport by the molecular motion. However, the turbulent viscosity/eddy viscosity ν_t , in contrast to the molecular viscosity ν , is not a fluid property but depends strongly on the state of turbulence. ν_t may vary significantly from one point in the flow to another and also from flow to flow.

Because the eddy viscosity concept itself was frequently criticised as being physically unsound, the more complex stress/flux-equation models with more complete physical background and stronger ability in prediction were established (Chou 1945, Rotta 1951), which could be exercised numerically with the advent of electric computers (Hanjalic and Launder 1972). Reynolds stress models employ transport equations for the individual Reynolds-stress tensor $-\overline{\rho u_i u_j}$ or second-moment $\overline{u_i u_j}$. However, they must be modelled first to obtain a closed system. The derivation of the exact Reynolds stress transport equations has the special advantage of introducing conveniently terms accounting for buoyancy, rotational and other special effect (body-force generation).

Turbulence models based on the transport equations for $\overline{u_i u_j}$ are unfortunately more complex than those models based on the eddy viscosity concept, especially when they are to satisfy the requirements of invariance and realizability. Though theoretically turbulence Reynolds stress closure models have great potential, they are therefore not much in use for practical applications. One of the main reasons restricted the application of the high-class second-moment closure models is that, in early studies simulated by the Reynolds stresses models, the simplified wall treatment, called "law of the wall" or "wall-function approximation", had to be utilised. However, these assumptions are less likely to be valid for complex turbulent wall shear flows, as there are very many situations where the near-wall processes are too complex for the supposition of log-law and local-equilibrium boundary conditions to be adequate. Hence to investigate and develop further refined near-wall Reynolds-stress closures is really needed. A challenging work that the computations must be extended to the wall and, thus, the model of turbulence must be adapted to include viscous influences has been tentatively solved in the near few years. In 1989, Launder and Shima extended the widely used second-moment closure of Gibson and Launder (1978) so as to be applicable for the flat-plate boundary layer within the near-wall sub-layer where viscous effects are substantial.

In principle, there is no need to adopt special practices for turbulent flows, for the Navier-Stokes equations apply equally to a turbulent motion as to a laminar one. All that is required is a computer program to solve numerically the equation in a supercomputer with enough storage and high computational speed. Though there still has a long distance for adopting DNS in engineering computations of turbulence, the DNS of simple shear flows, however, has proven to be an effective and important tool for studying turbulence structures and near-wall effects. At present, it is possible to examine the individual behaviours of some important terms of the second-moment turbulence models by using the results from DNS. Shin and Lumley (1993) has compared some second-moment closures to those of the DNS of homogeneous turbulence. Therefore, it has become demanding but necessary tasks for us to compare second-moment closures to the numerical simulation results of DNS in inhomogeneous turbulence, such as in channel flow (Huser and Biringen 1996).

A frequently encountered situation of turbulent shear flows, the flat-plate boundary layer flow, was chosen in the present research as the tested flow case. A database from the DNS of the flat-plate boundary layer turbulent flow was employed to investigate numerically

the ability of the L&S-Model for modelling near-wall sub-layer of turbulence. The fundamental governing equation, numerical method and main results are simply reported in the paper.

2. FUNDAMENTAL EQUATIONS

For the classical incompressible, steady flat-plane boundary layer flow under a Cartesian co-ordinate system $(x_1x_2x_3)$, the equations of mean movement can be expressed as follows

$$\frac{\partial U_1}{\partial x_1} + \frac{\partial U_2}{\partial x_2} = 0 \quad (1)$$

$$\frac{\partial(U_1^2)}{\partial x_1} + \frac{\partial(U_1U_2)}{\partial x_2} = \frac{\partial}{\partial x_2} \left(\nu \frac{\partial U_1}{\partial x_2} - \overline{u_1u_2} \right) \quad (2)$$

where x_1 stands for the longitudinal direction, x_2 represents the normal direction and x_3 denotes the lateral direction, respectively.

The second-moment $\overline{u_1u_2}$ can be solved by following transport equation

$$\frac{D}{Dt} \overline{u_1u_2} = P_{12} + \phi_{12} - \epsilon_{12} + d_{12}^v + d_{12} \quad (3)$$

where $\frac{D}{Dt} = \frac{\partial}{\partial t} + U_k \frac{\partial}{\partial x_k}$; U_i and u_i stand for the mean velocity and corresponding fluctuating quantity; ν is the kinematic viscosity.

In order to determine turbulent kinetic energy $k = \frac{1}{2} \overline{u_iu_i}$, three normal stress transport equations, except for the equations (1)-(3), also need to be solved by following equations

$$\frac{D}{Dt} \overline{u_1^2} = P_{11} + \phi_{11} - \epsilon_{11} + d_{11}^v + d_{11} \quad (4)$$

$$\frac{D}{Dt} \overline{u_2^2} = P_{22} + \phi_{22} - \epsilon_{22} + d_{22}^v + d_{22} \quad (5)$$

$$\frac{D}{Dt} \overline{u_3^2} = P_{33} + \phi_{33} - \epsilon_{33} + d_{33}^v + d_{33} \quad (6)$$

The dissipation rate ϵ_{ij} is defined by the assumption of local isotropy

$$\epsilon_{ij} = \frac{2}{3} \delta_{ij} \epsilon \quad (7)$$

where the δ_{ij} represents the Kronecker's delta. The components of dissipation rate ϵ_{ij} are given by

$$\epsilon_{11} = 2\epsilon / 3 \quad \epsilon_{22} = 2\epsilon / 3 \quad \epsilon_{33} = 2\epsilon / 3 \quad \epsilon_{12} = 0$$

The energy dissipation rate of turbulence ϵ is obtained by solving following transport equation

$$\frac{D\epsilon}{Dt} = \frac{\partial}{\partial x_k} \left[\left(c_\epsilon \frac{k}{\epsilon} \overline{u_k u_l} + \nu \delta_{kl} \right) \frac{\partial \epsilon}{\partial x_l} \right] + (c_{\epsilon 1} + \psi_1 + \psi_2) \frac{\epsilon}{k} P - c_{\epsilon 2} \frac{\epsilon}{k} \tilde{\epsilon} \quad (8)$$

where the shear production rate of turbulence energy $P = P_{kk} / 2$, empirical coefficients c_ϵ , $c_{\epsilon 1}$ and $c_{\epsilon 2}$ are 0.18, 1.45 and 1.9, $\tilde{\epsilon} = \epsilon - 2\nu \left(\frac{\partial k^{1/2}}{\partial x_j} \right)^2$, $\psi_1 = 2.5A \left(\frac{P}{\epsilon} - 1 \right)$ and $\psi_2 = 0.3(1 - 0.3A_2) \exp[-(0.002R_t)^2]$, respectively. The turbulence Reynolds number $R_t = k^2 / \nu \epsilon$ and stress flatness factor $A = [1 - 9(A_2 - A_3) / 8]$, A_2 and A_3 are two independent Reynolds stress invariants, *i.e.*,

$$\text{the second invariance of } a_{ij} \quad A_2 = a_{ik} a_{ki}$$

$$\text{and the third invariance of } a_{ij} \quad A_3 = a_{ik} a_{kj} a_{ji}$$

where $a_{ij} = (\overline{u_i u_j} - 2\delta_{ij} k / 3) / k$ is the dimensionless anisotropic part of the Reynolds stress, which is a proposal first made by Rotta in 1951.

Since the stress generation rate by mean shear P_{ij} and the viscous diffusion rate d_{ij}^v require no approximation and the turbulence diffusion of stress d_{ij} usually adopts the generalised gradient diffusion hypothesis, one can easily derive their component expressions

$$P_{11} = -2\overline{u_1 u_2} \frac{\partial U_1}{\partial x_2} \quad P_{22} = -2\overline{u_2^2} \frac{\partial U_2}{\partial x_2} \quad P_{33} = 0 \quad P_{12} = P_{21} = -\overline{u_1 u_2} \frac{\partial U_2}{\partial x_2} - \overline{u_2^2} \frac{\partial U_1}{\partial x_2}$$

$$\text{and} \quad d_{11}^v + d_{11} = \frac{\partial}{\partial x_2} \left[\left(C_s \frac{k}{\epsilon} \overline{u_2^2} + \nu \right) \frac{\partial \overline{u_1^2}}{\partial x_2} \right] \quad d_{22}^v + d_{22} = \frac{\partial}{\partial x_2} \left[\left(C_s \frac{k}{\epsilon} \overline{u_2^2} + \nu \right) \frac{\partial \overline{u_2^2}}{\partial x_2} \right]$$

$$d_{33}^v + d_{33} = \frac{\partial}{\partial x_2} \left[\left(C_s \frac{k}{\epsilon} \overline{u_3^2} + \nu \right) \frac{\partial \overline{u_3^2}}{\partial x_2} \right] \quad d_{12}^v + d_{12} = \frac{\partial}{\partial x_2} \left[\left(C_s \frac{k}{\epsilon} \overline{u_2^2} + \nu \right) \frac{\partial \overline{u_1 u_2}}{\partial x_2} \right]$$

The averaged product of the fluctuating pressure and strain fields (pressure-strain rate tensor) $\phi_{ij} \equiv \frac{1}{\rho} \overline{p(u_{ij} + u_{ji})}$ can be divided into four distinct terms for modelling near-wall sub-layer, namely the slow, rapid, slow wall-reflection and rapid wall reflection terms, respectively

$$\phi_{ij} = \phi_{ij1} + \phi_{ij2} + \phi_{ij1}^w + \phi_{ij2}^w \quad (9)$$

where the last two terms in the right-hand side, *i.e.*, the wall reflection terms ϕ_{ij1}^w and ϕ_{ij2}^w , usually have variable and extremely complicated expresses in different models. For L&S-Model, the components of pressure strain term ϕ_{ij} can be written as

$$\phi_{111} = -c_1 \varepsilon a_{11} \quad \phi_{221} = -c_1 \varepsilon a_{22} \quad \phi_{331} = -c_1 \varepsilon a_{33} \quad \phi_{121} = -c_1 \varepsilon a_{12}$$

$$\phi_{112} = -c_2 (P_{11} - 2P/3) \quad \phi_{222} = -c_2 (P_{22} - 2P/3) \quad \phi_{332} = -c_2 (P_{33} - 2P/3)$$

$$\phi_{122} = -c_2 P_{12}$$

$$\phi_{111}^w = \phi_{221}^w = \phi_{331}^w = c_1^w \overline{\varepsilon u_2^2} f / k \quad \phi_{121}^w = -3c_1^w \overline{\varepsilon u_1 u_2} f / 2k$$

and $\phi_{112}^w = \phi_{222}^w = \phi_{332}^w = c_2^w \phi_{222} f$ $\phi_{122}^w = -3c_2^w \phi_{122} f / 2$

where the near-wall damping function $f = 0.4k^{3/2} / \varepsilon x_2$, x_2 stands for the distance normal to the wall. The recommended forms of the coefficients $c_1 = 1 + 2.58AA_2^{1/4} \left(1 - \exp\left[-(0.0067R_t)^2\right]\right)$, $c_2 = 0.75A^{1/2}$, $c_1^w = -2c_1 / 3 + 1.67$ and $c_2^w = \max\left[(2c_2 / 3 - 1 / 6) / c_2, 0\right]$, respectively.

3. NUMERICAL METHOD

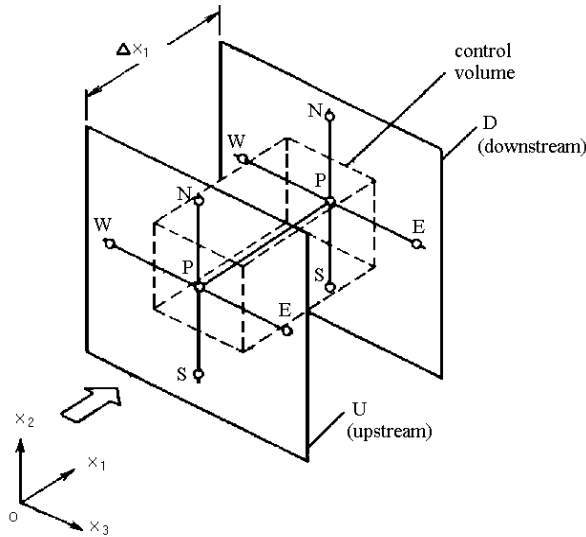


Figure 1- Control volume adopted to obtain finite-difference equation.

A numerical calculation procedure for momentum, heat and mass transfer in three dimensional parabolic flows (Patankar and Spalding, 1971) has been used to compute fundamental governing equations. For this kind of flows, the co-ordinate in the main flow direction (x_1) becomes a “one-way” co-ordinate, *i.e.*, the upstream conditions can determine

the downstream flow properties, but not vice versa. Such flows give rise to parabolic differential equations, in a more general sense, also called boundary-layer flows. It is a convenient behaviour of the boundary-layer flows that enables us to employ a marching integration from an upstream station to a downstream one. The fundamental governing equations of fluid movement and transport for boundary-layer flows in a Cartesian coordinate system $x_1x_2x_3$ can be generally written by following form

$$\frac{\partial}{\partial x_1}(\rho U_1 \phi) + \frac{\partial}{\partial x_2}(\rho U_2 \phi) + \frac{\partial}{\partial x_3}(\rho U_3 \phi) = \frac{\partial}{\partial x_2} \left(\Gamma_\phi \frac{\partial \phi}{\partial x_2} \right) + \frac{\partial}{\partial x_3} \left(\Gamma_\phi \frac{\partial \phi}{\partial x_3} \right) + S_\phi \quad (10)$$

where Γ_ϕ stands for the transport property such as viscosity in momentum equations. The source-sink term S_ϕ on the right-hand side should include all terms which can not be expressed in the forms of convection and diffusion. By integrating equation (10) over the control volume shown in the Fig. 1 by dotted lines, one can transform it into a discretized algebraic expression

$$\phi_P = A_N^\phi \phi_N + A_S^\phi \phi_S + A_E^\phi \phi_E + A_W^\phi \phi_W + B^\phi \quad (11)$$

where A_N , A_S , A_E and A_W stand for coefficients, B^ϕ represents source term. The finite-difference equation like (11) can be solved by successive use of the TDMA (*Tri-Diagonal Matrix Algorithm*) in the x_2 and x_3 directions. The foregoing procedure for calculation was based on the assumption that the longitudinal pressure gradient ($\partial \bar{p} / \partial x$) is taken to be the same as the longitudinal pressure gradient prevailing in the irrotational free stream adjacent to the boundary layer. Then the solution of momentum equation for u_1 is straightforward. The numerical calculation was carried out for a flat-plate boundary layer with the Reynolds number being 8,000 and 175 nodal grads along the computational altitude. The adopted longitudinal forward step length Δx_1 equals to 10^{-4} m and the molecular viscosity ν is 1.48×10^{-5} m²/s, respectively.

4. COMPARISONS

By use of the foregoing procedure, the authors calculated the incompressible, steady flat-plate boundary layer turbulent flow, closed by Launder & Shima's Model (L&S-Model). The computation employed the no-slip condition at the wall, instead of the frequently used law of the wall (wall-function approximation) at the region close to the rigid surface, at the wall-adjacent nodes. Figures 2 - 7 present the comparisons of the data resulted from DNS, represented by circle-dots, with those resulted from L&S-Model, represented by real lines, while the number of forward steps (NFS) equals to 10^4 . In order to clarify and analyse conveniently the distributions across the near-wall sub-layer, the logarithmic abscissa (in the normal direction of the flat-plate boundary layer) was adopted in these figures to illustrate the non-dimensional distance to the wall y^+ , where $y^+ = yU_w/\nu$, U_w stands for the friction velocity. The ordinates in Figures 2-7 are the dimensionless longitudinal velocity U_1/U_w , dimensionless turbulent shear stress $\overline{u_1 u_2}/U_w^2$, dimensionless turbulence intensities in longitudinal direction (x_1 -direction) $\overline{u_1^2}/U_w^2$, in vertical direction (x_2 -direction) $\overline{u_2^2}/U_w^2$ and in spanwise direction (x_3 -direction) $\overline{u_3^2}/U_w^2$ as well as the dimensionless dissipation rate of turbulent kinetic energy $\varepsilon^+ = \varepsilon\nu/U_w^4$, respectively.

The results computed by L&S-Model coincide quite well with those resulted from DNS, especially in the distributions of mean-velocity (see Fig. 2) and in the distributions of three normal stresses (see Figures 4-6), but except for the distributions of the dissipation rate of turbulence kinetic energy ε^+ in the range of $y^+ < 80$ (see Fig. 7). The profile of ε^+ , calculated by L&S-Model, seems to be unreasonable, while a peak value of ε^+ appears at $y^+ = 10$, the value of ε^+ within the range of $8 < y^+ < 80$ was over-predicted and also the value of ε^+ in the range of $y^+ < 10$ decreases along with the decrease of the non-dimensional distance to the wall y^+ . The profile of ε^+ shown by the database from DNS (Direct Numerical Simulation), which can not be provided by the laboratory measurement, presents a different tendency that ε^+ continuously increases to the wall till $y^+ = 0.3$ but without the appearance of a peak value at $y^+ = 10$. The difference of the distributions of ε^+ , resulted from L&S-Model and DNS, may be caused by the assumption of local isotropy (see equation 7), simply adopted by the L&S-Model. Also, the assumption of local isotropy may make some difference of turbulence shear stresses distributions in the range of $1 < y^+ < 10$ (see Fig. 3), while the production of turbulence calculated by L&S-Model is larger than the data resulted from DNS, though these two profiles in the other ranges ($y^+ < 1$ and $y^+ > 10$) are well agreed each other.

5. CONCLUSIONS

DNS is a useful tool which can provide detailed database for investigating numerically the behaviours of RSM, especially to extend the second-moment closure to the near-wall sub-layer.

Generally speaking, L&S-Model is a good second-moment closure model which can simulate and predict various turbulence quantities in the region of near-wall sub-layer, except for the dissipation rate of turbulence kinetic energy.

It is possible to improve further L&S-Model by use of some non-isotropic forms of the dissipation rate of turbulence kinetic energy, instead of the simple assumption of local isotropy.

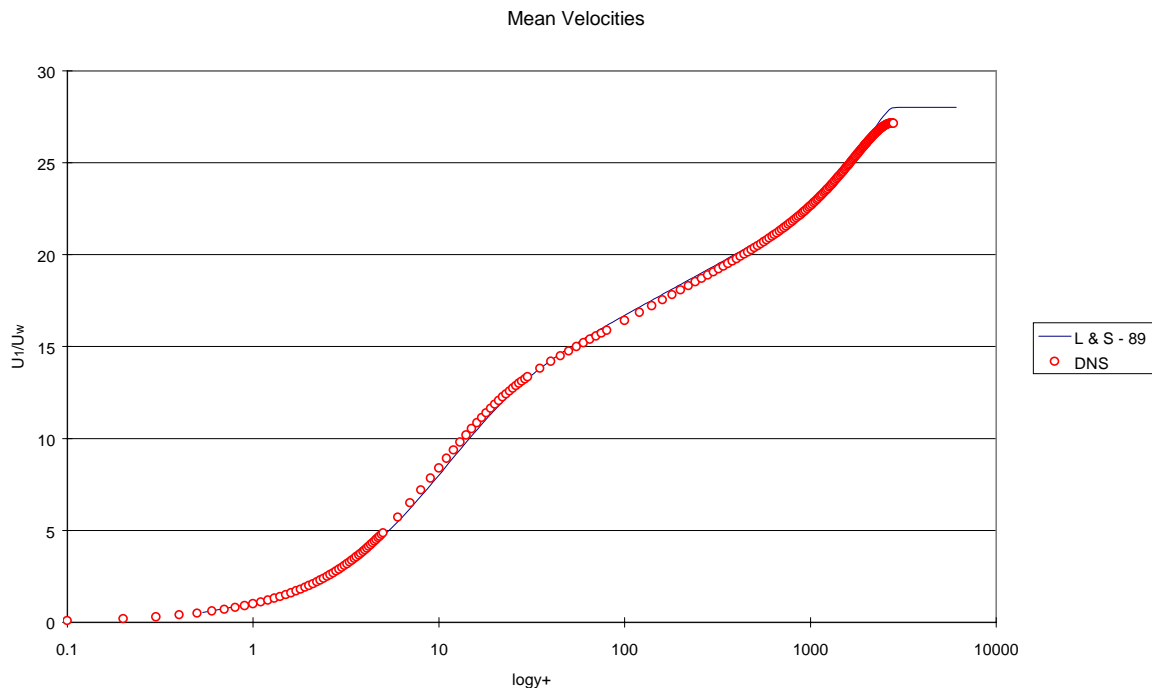


Figure 2- Mean velocity (NFS= 10^4).

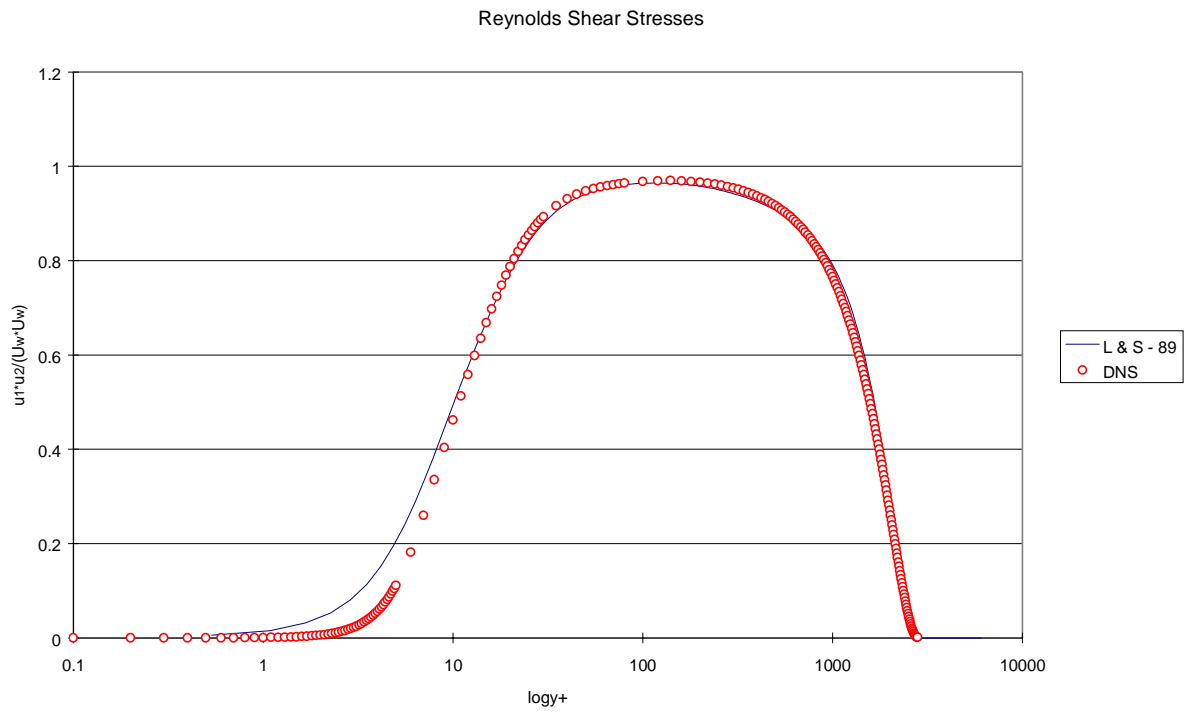


Figure 3- Turbulent shear stress ($NFS=10^4$).

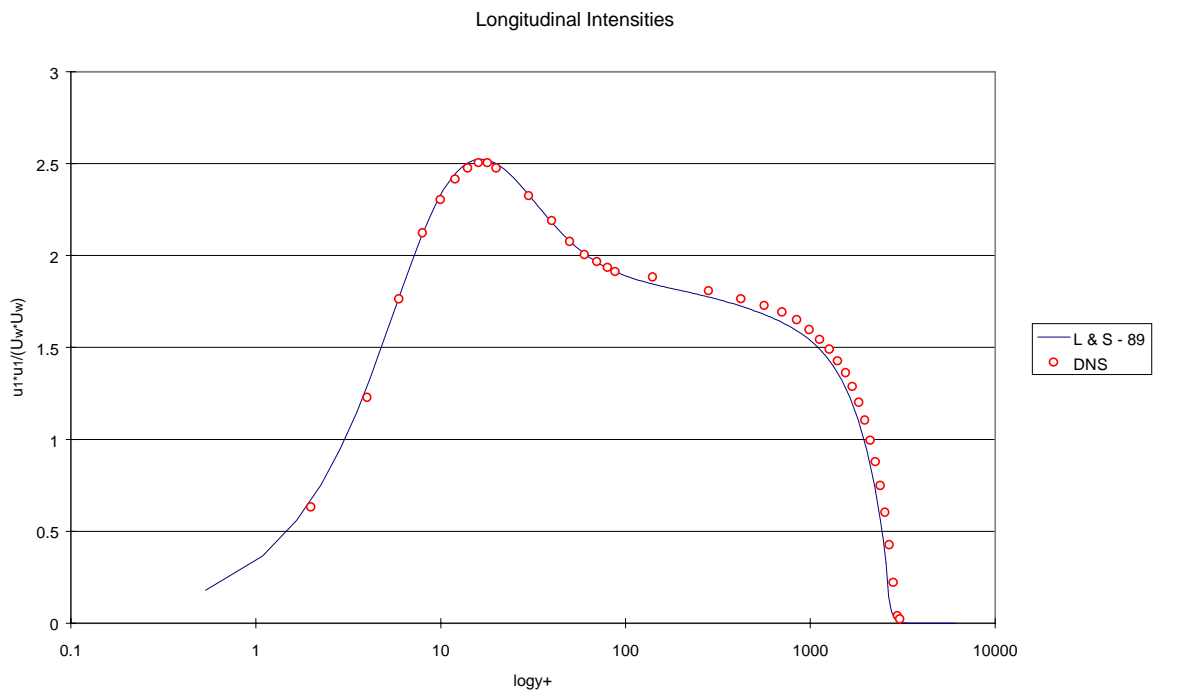


Figure 4- Longitudinal turbulent intensity ($NFS=10^4$).

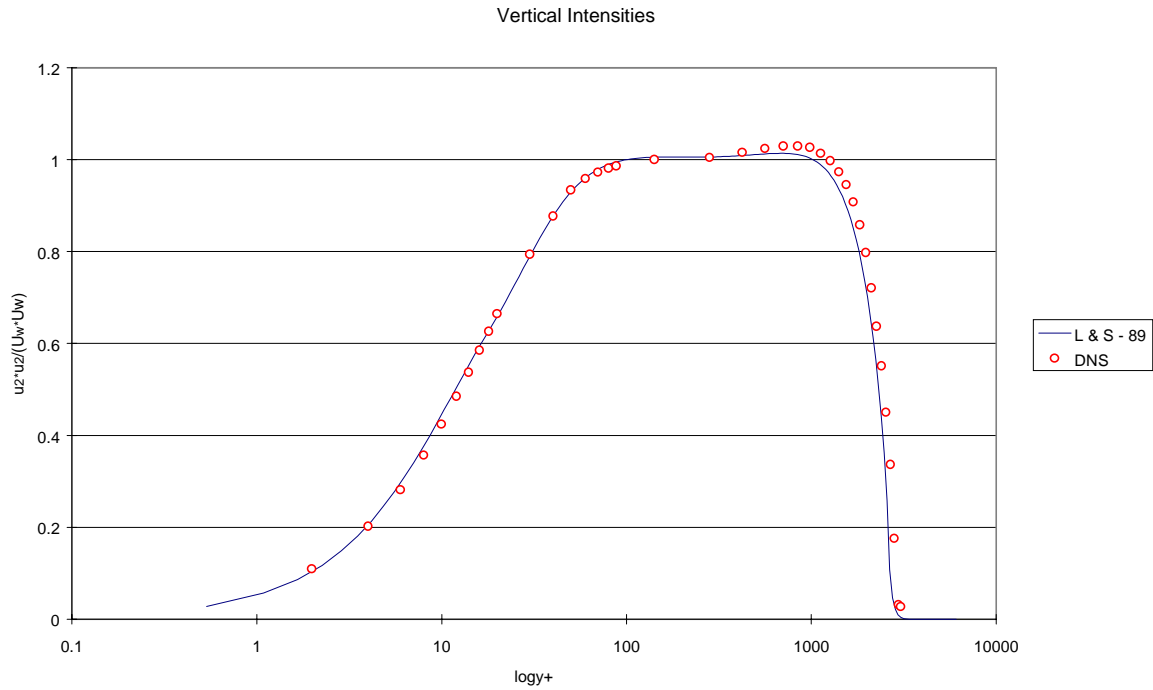


Figure 5- Vertical turbulent intensity ($NFS=10^4$).

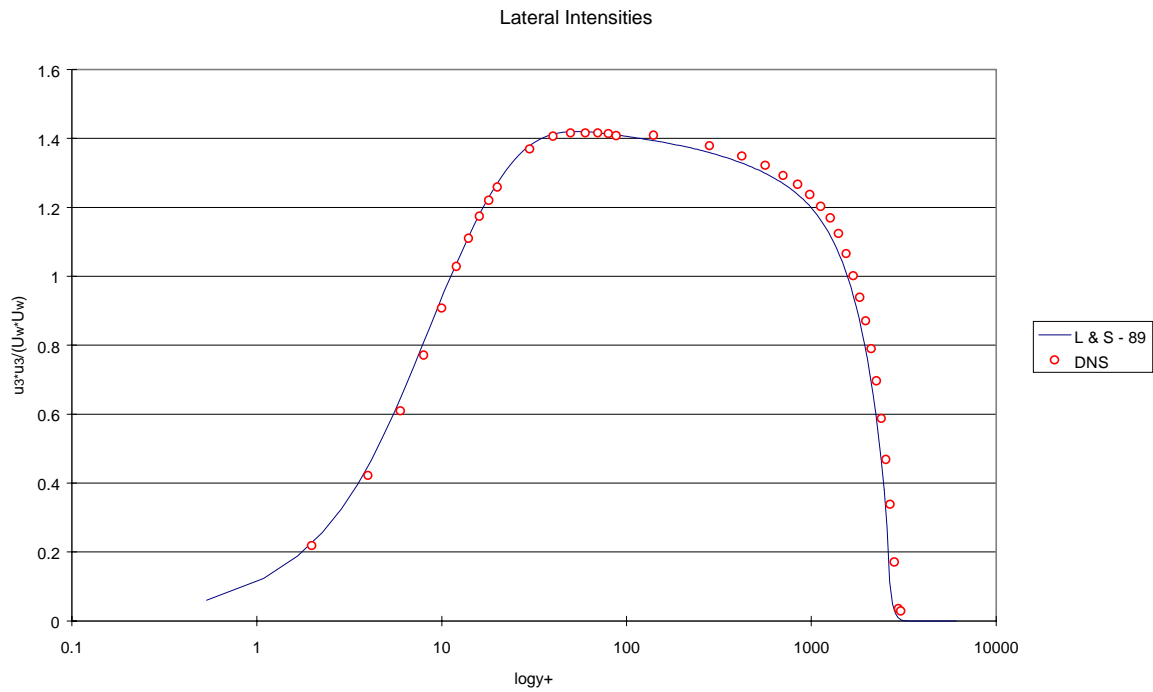


Figure 6- Lateral turbulent intensity ($NFS=10^4$).

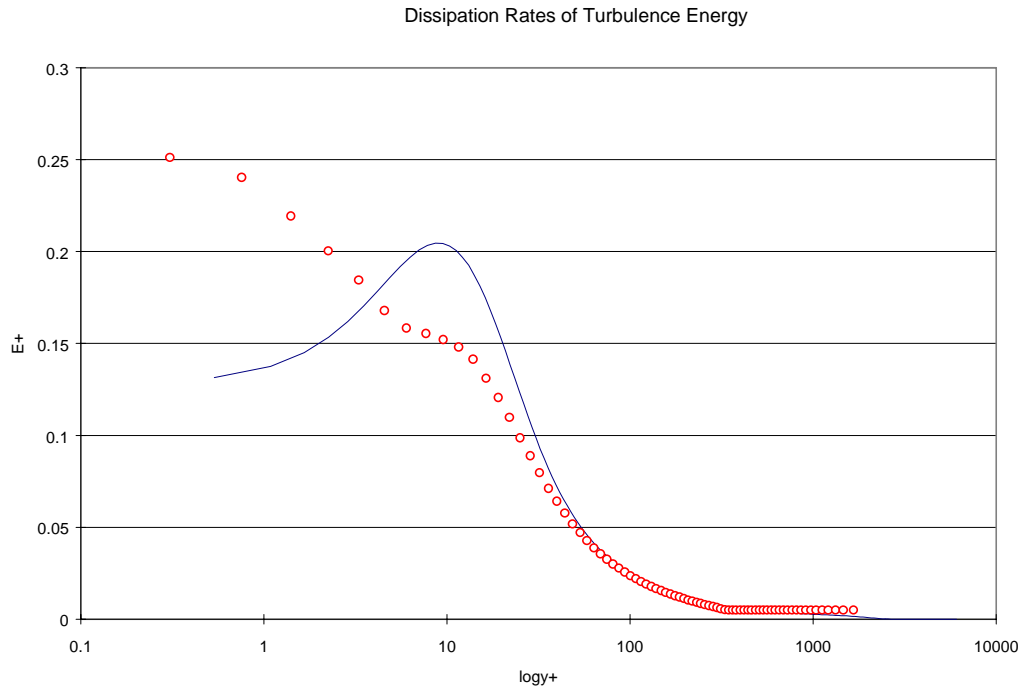


Figure 7- Dissipation rate of turbulence kinetic energy ($NFS=10^4$).

Acknowledgement

The support of FAPESP (*Foundation for Supporting Research at São Paulo State*) through the Project No. 1997/13955-4 is gratefully acknowledged.

REFERENCES

- Chou, P. Y.,1945, On the velocity corrections and the solution of the equations of turbulent fluctuation, *Quart. Appl. Math.* Vol. 3, 38-
- Gibson, M. M. & Launder, B. E.,1978, Ground effects on pressure fluctuations in the atmospheric boundary layer, *Journal of Fluid Mechanics*, Vol. 86, pp. 491 -.
- Hanjalic, K. & Launder, B. E.,1972, A Reynolds-stress model of turbulence and its application to thin shear flows, *Journal of Fluid Mechanics*, Vol. 52, pp. 609-.
- Huser, A. & Biringen, S.,1996, Simulation of turbulent square-duct flow: dissipation and small-scale motion, *AIAA Journal*, Vol. 34 n. 12, pp. 2509-2513.
- Launder, B. E. & Shima, N.,1989, Second-moment closure for the near-wall sublayer: development and application, *AIAA Journal*, Vol. 27, n. 10, pp. 1319-1325.
- Patankar, S. V. & Spalding, D. B.,1972, A calculation procedure for heat, mass and momentum transfer in three-dimensional parabolic flows, *International Journal of Heat and Mass Transfer*, Vol. 15, pp. 1787-806.
- Rotta, J.,1951, Statistische theorie nichthomogener turbubulenz, *Zeitsch. für Physik*, Vol. 129, pp. 547-572 and Vol. 131, pp. 51-77.
- Shin, T. H. & Lumley, J. L.,1992, Kolmogorov behavior of near-wall turbulence and its application in turbulence modelling, NASA TM-105663, ICOMP-92-06.